Electron scattering by highly polar molecules

B. Jaduszliwer, A. Tino,* and B. Bederson
Physics Department, New York University, New York, New York 10003
(Received 19 April 1984)

We have measured effective cross sections for the scattering of electrons by CsBr, RbBr, CsCl, RbCl, and KI, using the molecular-recoil technique, in the 1—22.5-eV energy range. We show that these can be expressed as an integral of the differential cross section folded with an apparatus form factor, which has the effect of suppressing the very large small-angle contribution to scattering. The apparatus form factor is calculated explicitly, and a precise prescription for comparison with theory is given. The data are compared with calculations using the rotating-dipole first Born approximation and semiclassical perturbation theory [A. S. Dickinson, J. Phys. B 10, 967 (1977)] differential cross sections.

I. INTRODUCTION

The scattering of electrons by molecules possessing a permanent dipole moment has been of interest to physicists for more than 50 years. The dipole interaction is the longest-range interaction possible between a point charge and a neutral system, and it can be expected to dominate scattering at long distances. Modeling the molecule by a rotating dipole leads to quite simple results for the scattering cross sections, which in turn can be used as the conceptual basis for more elaborate calculations. Massey used this model, and in 1931 calculated[1] the differential cross section for the scattering of an electron by a rotating point dipole in the first Born approximation (RPDFBA). Following this approach leads to very large cross sections, very strongly peaked in the forward direction, and dominated by rotationally inelastic processes with $\Delta j = \pm 1$. In the limit of infinite molecular moment of inertia (i.e., fixed, rather than rotating, dipole), the differential cross section becomes divergent in the forward direction.

For the first 40 of these 50 years, the only experimental data available on electron—polar-molecule scattering were measurements of drift velocities of electrons moving in a dense polar gas under the influence of electric fields,[2–7] using "swarm" techniques, first introduced by Townsend and Bailey.[8] Momentum-transfer cross sections can be inferred from those measurements by means of a quite involved analysis using transport theory, which becomes even more complicated in this molecular case because inelastic collisions are dominant.

In an effort to simplify the analysis of those experiments, Altshuler[9] used an adiabatic approximation to treat the inelastic collision with a rotating dipole as an angle-averaged elastic collision with a fixed dipole; he used the first Born approximation to treat this problem, and then computed momentum-transfer cross sections for electrons scattering on H_2O and NH_3 which were in reasonable agreement with the existing experimental results.[2] Mittleman and von Holdt[10] solved the same problem exactly, obtaining differential cross sections which were substantially larger than the Born results for large values of the dipole moment, and momentum-transfer cross sections which were further away from experiment than Altshuler's. Takayanagi[11] and Crawford[12] studied electron scattering by a rotating point dipole in the first Born approximation. The former calculated RPDFBA cross sections for rotational and vibrational excitation of linear molecules, while the latter calculated rotational excitation RPDFBA cross sections for linear, symmetric top and asymmetric top molecules. Crawford *et al.*[13] discussed the difficulties inherent in the adiabatic approach, generalized the definition of the momentum-transfer cross section, and analyzed the results of electron swarm experiments performed in a large number of weakly polar gases. Some pathological features characteristic of electron scattering by dipole fields (fixed or rotating, point or finite) were examined in great detail by various workers,[14–21] and the different roles played by the long-range nature of the interaction and the singularity at the origin were clarified. Crawford *et al.*[13] pointed out that for large values of the dipole moment the RPDFBA amplitudes may depart significantly from the unitarity constraint.

In the last ten years a number of more rigorous theoretical studies have been carried out, involving both fully quantum-mechanical and semiclassical calculations, following many different approaches both to represent the electron-molecule interaction and to solve the scattering problem. Reviews by Itikawa,[22] Lane,[23] and Norcross and Collins[24] discuss these approaches in detail and provide an extensive bibliography. This surge in activity was stimulated partly by the role played by electron—polar-molecule scattering in a variety of applications, primarily magnetohydrodynamic power generation, but also including gas lasers development and modeling, physics of the interstellar medium, physics of flames, etc.

Another powerful stimulant was the availability, for the first time, of scattering data obtained in crossed-beam experiments. Stern and collaborators[25–27] measured the angular distribution of CsF, CsCl, and KI molecules recoiled in collisions with electrons. As discussed below, the finite width of the molecular beam and electron and molecule momentum distributions, combined with the strong forward peaking of the angular distribution of scattered electrons, makes it impossible to directly extract electron scattering cross sections from the distribution of

recoiled molecules. Instead, Stern and collaborators produced computer fits to these angular distributions, using the known momentum distributions for the electron and molecular beams and the geometries of the overlap volume and the detector. The kinematics of the electron-molecule collision then allow the calculation of the distribution of recoiled molecules for a given electron differential scattering cross section; a six-term model cross section was used[28] and least-squares fits to the data yielded the six linear coefficients. The model cross sections thus determined were presented as the result of the experiment; they were also used to calculate total and momentum-transfer cross sections by straightforward integration.

In general their differential cross sections peaked more sharply in the forward direction than in the RPDFBA results, and they were much smaller than the RPDFBA everywhere. Unexpected minima were present at $\theta \simeq 60°-90°$ and $\theta \simeq 180°$.

Collins and Norcross[29] pointed out that the total cross sections calculated integrating those "best-fit" differential cross sections are smaller than the integral of the RPDFBA between 0° and 15°. This is a serious problem, since the RPDFBA is expected to be reasonably accurate in that range. They then suggested that the particular choice of model cross section by Stern and co-workers was a poor one, and that the data should be reanalyzed in terms of better models.

Trajmar, Srivastava, Vuskovic, and others at Jet Propulsion Laboratory measured relative differential cross sections for electrons scattering quasielastically on KI,[30] LiF,[31] and CsCl.[32] The general shape of their angular distributions was closer to expectations, but they had to be normalized to theory. In the case of KI, the data were normalized at 15° to a distorted-wave calculation described in the same paper; for LiF, the data were normalized to the semiclassical results of Dickinson[33] at 40°, and for CsCl at 15° to a calculation by Siegel *et al.*,[34] which at that angle is in good agreement with Dickinson's semiclassical results.[33] Electron energy-loss spectra for electronic excitations were also measured, and some excited-state potential energy curves in the Frank-Condon region were inferred from the analysis of the energy-loss spectra. In these experiments, the need to normalize the measured angular distribution to theory introduces a certain degree of arbitrariness, particularly since normalization has to be performed at relatively large angles, for which the discrepancies between different calculations are large.

In a recent paper[35] we described an experiment to study electron scattering on CsBr, yielding results which are independent of any normalization or cross-section modeling, and thus are a benchmark against which theory can be tested. In the present paper we extend the technique to CsCl, RbBr, RbCl, and KI. The experiments are described in Sec. II; the relationship between experimental results and relevant cross sections is discussed in Sec. III, and our results are presented in Sec. IV.

II. THE EXPERIMENT

The measurements have been performed using a new atomic and molecular beams apparatus at New York University, which has been described in detail elsewhere.[36] Briefly, the apparatus consists of a large source chamber, an intermediate chamber which for the purpose of this experiment is largely irrelevant, the interaction chamber, a long drift tube, and the detector chamber. The beam system is 5 m long. The experiments are performed using the molecular-recoil technique, in which post-collisional observations are made on the recoiled molecules, rather than the scattered electrons. Since molecular-recoil angles are small compared to electron scattering angles, high angular resolution is required, which in turn demands long geometry and good collimation of the molecular beam.

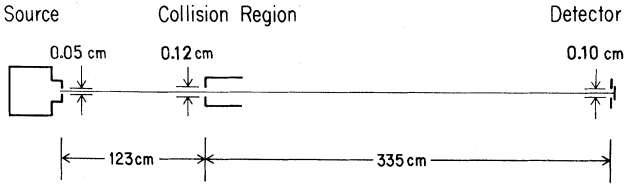

FIG. 1. Geometry of the experiment.

The geometry of the experiment is shown in Fig. 1. The alkali-halide beam is produced in a stainless-steel effusive source divided into two chambers; the first is a large cylinder, 220 cm^3 in volume, which contains the alkali halide under study, and the second is a snout made of a standard stainless-steel capped pipe fitting. The source nests snugly inside the cylindrical stainless-steel oven, heated by a MgO-insulated, stainless-steel-clad nichrome wire heater (a sketch of the oven assembly is contained in Ref. 36). Within the oven, a smaller superheater of similar design surrounds the source snout, allowing it to be maintained at a higher temperature than the molten alkali-halide container, so that the dimer fraction in the beam can be reduced substantially. Two wells fitted with chromel-allumel thermocouples are provided, one for the main heater and the other one for the snout superheater. Independent proportional temperature controllers supply the power for the heaters, and the feedback loops have been carefully adjusted to avoid temperature oscillations. The oven fits inside a triple heat shield which in turn is surrounded by a water-cooled jacket. A removable cover and triple heat shield close the opening at the back end; at the front end there is a water-cooled plate with a 0.32-cm orifice for the molecular beam. This plate also supports a triple heat shield, with a 1-cm hole for the beam. This geometry allows for most of the excess material effusing from the oven to condense immediately on the cold plate, thus preventing the broadening of the beam by scattering on a gas cloud in front of the source orifice.

The molecular beam source described above operates reliably for several hundred hours at temperatures of about 800 °C without reloading. Temperature differentials of up to 80 °C can be maintained routinely between the container and the snout.

In the interaction region the molecular beam is crossfired by a ribbon-shaped electron beam, produced by a modified version of the electron gun described by Collins *et al*;[37] a sketch of the gun is contained in Ref. 36. It consists of a stack of planar components aligned by four accurately located ceramic rods, and separated by alumi-

num oxide insulators. The oxide cathode is of the type used in 4D32 vacuum tubes, and it is indirectly heated. All metal components exposed to the electron beam are made out of molybdenum. The slits defining the electron beam at the overlap volume are 2.54 cm long and 0.08 cm high; a collimating slit, 0.118 cm high and 0.115 cm wide, mounted on the gun support block 1 cm upstream from the entrance to the collision region, defines the molecular beam at the overlap volume.

The voltages applied at the different electrodes are chosen so as to avoid strong focusing, thus making the electron trajectories almost perpendicular to the planar electrodes. The electron energy distribution can be measured using a retarding field technique, and it is about 0.5 eV full width at half maximum (FWHM); this relatively broad spread is adequate to the present experiment which is intended for the proposed study in potential scattering. The electron energy in the collision region is corrected for space charge and contact potential difference in the manner described by Collins *et al.* A large, double-walled high-permeability shield keeps the magnetic field in the volume occupied by the electron gun well below 10^{-2} G.

After traveling down a 3-m-long field-free drift tube, the molecules are dissociated and the alkali-metal constituent is surface-ionized on a 1-mm^2 hot platinum surface. The resulting positive ions are mass-analyzed in a 90° sector magnet, and after exiting, are collected in the cone of a high-current Channeltron electron multiplier operating in the analog (low-gain) mode.

The detector can be displaced in the plane normal to the beam axis, so that the two-dimensional molecular-beam intensity profile can be measured, with and without scattering. Figure 2 shows the vertical and horizontal profiles for an unscattered RbCl beam. They follow very closely the trapezoidal ones calculated from the apparatus geometry.[38] These profiles are highly reproducible over extended periods of time, even after changing molecular species.

The Channeltron output current is measured using a high-sensitivity electrometer, whose voltage output is sampled periodically by the analog-to-digital converter of a PDP 11/03 computer controlling the experiment. The electron gun is turned alternatively on and off by the PDP 11/03 digital-to-analog converter feeding a positive or negative voltage to the first slit in the electron gun. The

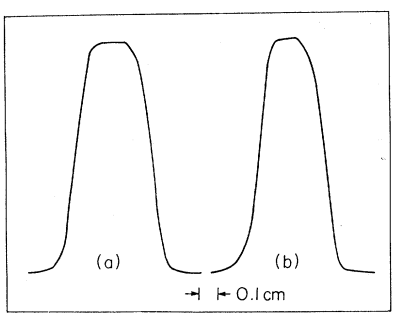

FIG. 2. Measured plots of molecular beam intensity profiles. (a) Horizontal, (b) vertical. These plots follow very closely the theoretical ones obtained by folding the calculated trapezoidal beam current density profiles with the 0.01-cm^2 square detector.

corresponding molecular beam signals at the detector, I_{on} and I_{off}, are recorded. In these experiments the detector is set on the flat top of the molecular-beam intensity profile, near the leading edge of the molecular beam as seen by the electrons. The quantity that we measure is[39] the effective cross section for scattering out of the detector,

$$\Delta\sigma = \frac{h\bar{V}}{I_e}\frac{I_{off}-I_{on}}{I_{on}}\ , \tag{1}$$

where $\bar{V}=[\int \mathcal{V}(V)V^{-1}dV]^{-1}$; $\mathcal{V}(V)$ is the molecular speed distribution in the beam. For a Maxwellian beam, $\bar{V}=(8kT/\pi M)^{1/2}$. h is the height of the beam overlap volume, and I_e is the electron number current. Since only a ratio of molecular beam intensity measurements appears in Eq. (1), knowledge of the absolute efficiency of the molecular detector is not required. The experiment will yield an absolute measurement of $\Delta\sigma$ provided that care is taken to eliminate backscattering on secondary emission from the electron-gun anode, and that all the electrons reaching the anode actually travel through the molecular beam. This ability to determine absolute values of cross sections represents one of the major advantages of the recoil technique.

In earlier work with atomic targets[39] $\Delta\sigma$, as determined by Eq. (1), was identified as the total scattering cross section. This assumes that the detector did not collect any of the atoms recoiled by very small angles, which of course is never strictly true. Bederson and Kieffer[40] examined this problem in detail, and for atomic targets this "scattering-in" contribution to $\Delta\sigma$ can in many cases be made negligible. In the case of polar molecules, since the forward contribution to the scattering cross section is large, the fraction of molecules collected by the detector after small-angle scattering, and thus not counted as scattering events, is large too. The problem is made worse if the molecular mass is large, because this has the effect of collapsing the full 4π angular distribution of scattered electrons into a very narrow cone of recoil angles for the molecules (approximately 2×10^{-4} sr for 10-eV electrons scattering on CsBr, as an example). Thus, the scattering-in contribution to $\Delta\sigma$ cannot be neglected. This is discussed in detail in Sec. III.

It is well known that dimers can constitute a significant fraction of an alkali-halide beam.[41] Miller and Kusch[42] measured the dimer fraction in alkali-halide beams, and obtained the corresponding dimer dissociation constants. We used their results to estimate the dimer fraction in our experiments, which was kept below 1% for CsBr and CsCl, and below 2.5% for KI, RbBr, and RbCl.

III. ANALYSIS OF THE EXPERIMENT

The relationships between molecular fluxes and recoil angles, which are the observables in the present experiment, and the center-of-mass electron scattering angles and differential cross sections were examined in detail in Ref. 36, and are only briefly summarized here. Figure 3 shows the molecular beam incident along the y axis (momentum $M\vec{V}$) and the electron beam incident along the z axis (momentum $m\vec{v}$). After the collision the molecule and electron momenta are $M\vec{V}'$ and $m\vec{v}'$. Defining

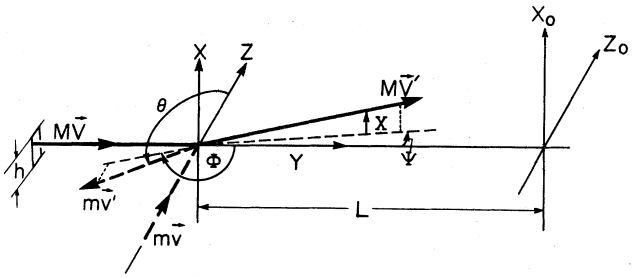

FIG. 3. $M\vec{V},M\vec{V}'$: molecular momenta before and after the collision. $m\vec{v},m\vec{v}'$: same for electron. θ,ϕ: electron scattering angles. ψ,χ: molecular-recoil angles. (x_0,z_0): detector plane. h, height of overlap volume. L, distance between collision region and detector plane.

$\alpha=mv/MV$ and $\beta=mv'/MV$, the molecular recoil angles ψ (in the plane of the beams) and χ (in the normal plane containing $M\vec{V}'$) are given by

$$\psi=\alpha-\beta_k\cos\theta\ , \tag{2}$$

$$\chi=\beta_k\sin\theta\sin\phi\ , \tag{3}$$

where the molecule is assumed to be initially in the electronic ground state, and after the collision is left in a state labeled by k. θ and ϕ are the electron scattering angles. These expressions are correct to first order in α,β. In the present experiments, the largest value of α is 0.05, making the second-order correction negligible. For elastic scattering, $\beta_k=\alpha$. For rotationally and vibrationally inelastic collisions, $\beta_k\simeq\alpha$, and so we will refer to them as quasielastic collisions.

When the electron gun is turned on, the number of molecules scattered per unit time out of their original trajectories leading to the detector is given by[39]

$$\Delta I_{\rm out}=I_eI_0\frac{Q(E_0)}{h\bar{V}}\ , \tag{4}$$

where I_0 is the number of molecules reaching the detector per unit time with the electron gun off, and $Q(E_0)$ the so-called "grand" total scattering cross section at electron energy E_0.

Figure 4 maps the molecular beam cross section at the detector plane. The electrons are incident from the left along the z axis, and the molecules are traveling into the

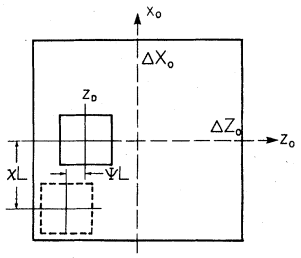

FIG. 4. Map of the molecular beam cross section at the detector plane. Square detector is at $x_0=0$, $z_0=z_D$. Molecules reaching the detector after being recoiled by ψ,χ would, in the absence of collisions, cross the detector plane at $x_0=-\chi L$, $Z_0=z_D-\psi L$.

paper. ΔX_0 and ΔZ_0 are the vertical and horizontal half-widths of the beam at the base, respectively, and the detector is set at $x_0=0$, $z_0=z_D$, at the flat top of the intensity profile. Jaduszliwer *et al.*[36] show that the number of molecules recoiled into the detector after scattering an electron elastically or quasielastically is given by

$$\Delta I_{\rm in}=\frac{2I_eI_0}{h}\int\frac{dV}{V}\mathscr{V}(V)\times\int_0^{\Delta\Theta}d\theta\sin\theta\,\sigma(E_0,\theta)\times\mathscr{G}(z_D-\alpha L+\alpha\cos\theta)\times\int_{-\Phi}^{\Phi}\mathscr{F}(-\alpha L\sin\theta\sin\phi)d\phi\ , \tag{5}$$

where $\mathscr{F}$ and $\mathscr{G}$ are the vertical and horizontal beam intensity profiles, normalized to unity at the top; the limits of integration are given by

$$\Phi=\pi/2\ \text{ if }\Delta X_0\geq\alpha L\sin\theta \tag{6a}$$

$$\Phi=\arcsin(\Delta X_0/\alpha L\sin\theta)\ \text{ if }\Delta X_0<\alpha L\sin\theta \tag{6b}$$

$$\Delta\Theta=\arccos[1-(z_D+\Delta Z_0)/\alpha L]\ . \tag{7}$$

L is the distance between the collision volume and the detector. The smallest recoil angle for electronically inelastic processes is given by $\psi=\alpha-\beta$, corresponding to forward ($\theta=0$) scattering. Molecules which have scattered an electron into the forward direction after an inelastic collision with energy loss E^* will be displaced by an amount z_0' as they cross the detector plane. For molecules with $V=\bar{V}=(8kT/\pi M)^{1/2}$

$$z_0'=\left[\frac{\pi}{4}\frac{m}{M}\right]^{1/2}L\frac{E_0^{1/2}-(E_0-E^*)^{1/2}}{(kT)^{1/2}}\ , \tag{8}$$

where T is the snout temperature. CsCl will yield the smallest value for z_0' in our experiments, which obtains for the highest electron energy we have investigated, $E_0=25$ eV. $E^*=4.96$ eV,[32] yielding $z_0'=0.98$ cm. This is much larger than the distance between the left edge of the molecular beam and the detector. Thus, the detector will not collect any molecules recoiled in electronically inelastic collisions; Eq. (5) will give the full scattering-in contribution to the scattering signal, $\Delta I=\Delta I_{\rm out}-\Delta I_{\rm in}$. If electronically inelastic processes can be neglected,[43] Eq. (4) for $\Delta I_{\rm out}$ can be rewritten as

$$I_{\rm out}=2\pi\bar{V}\int\frac{dV}{V}\mathscr{V}(V)\int_0^{\pi}\sigma(E_0,\theta)\sin\theta\,d\theta \tag{9}$$

and combining Eqs. (1), (5), and (9), with $I_{\rm on}=I_0$, we obtain

$$\Delta\sigma=\frac{\Delta I}{I_eI_0}h\bar{V}=2\pi\bar{V}\int\frac{dV}{V}\mathscr{V}(V)\int_0^{\pi}\sigma(E_0,\theta)\Gamma(\theta,E_0,V)\sin\theta\,d\theta\ , \tag{10}$$

where the scattering-out form factor $\Gamma(\theta,E_0,V)$ is given by

$$\Gamma(\theta,E_0,V)=1-\mathcal{G}(z_D-\alpha L+\alpha L\cos\theta)\gamma(\theta,E_0,V) \quad \text{if } \theta\leq\Delta\Theta \tag{11a}$$

$$\Gamma(\theta,E_0,V)=1 \quad \text{if } \theta>\Delta\Theta \tag{11b}$$

$\gamma(\theta,E_0,V)$ is the "azimuthal form factor"[36]

$$\gamma(\theta,E_0,V)=\frac{1}{\pi}\int_{-\Phi}^{\Phi}\mathcal{F}(-\alpha L\sin\theta\sin\phi)d\phi\ . \tag{12}$$

For very small scattering angles, $\gamma(\theta,E_0,V)\simeq 1$, and $\mathcal{G}(z_D-\alpha L+\alpha L\cos\theta)\simeq 1$ too, since the detector is set at the top of the trapezoidal intensity distribution. Then $\Gamma\simeq 0$. In a well-designed experiment, $\Delta\Theta\ll 1$. Clearly, if $\sigma(E_0,\theta)$ is not too sharp (i.e., if it is not much larger when $0\leq\theta\leq\Delta\Theta$ than elsewhere) then $\Delta\sigma\simeq Q(E_0)$. But that is not the case for the present experiments, as discussed in Sec. II. Comparison of our results with the theoretical calculation requires the use of Eq. (10) and evaluation of $\Gamma(\theta,E_0,V)$.

$\Delta\Theta$ is small enough in these experiments for the small-angle approximation for $\sin\theta$ and $\cos\theta$ to be used when evaluating Eq. (11a). Defining

$$\theta_0=\arcsin\left(\Delta X_0/\alpha L\right) \tag{13}$$

again, θ_0 is small, so that $\theta_0=\Delta X_0/\alpha L$. In the conditions of our experiments, $\Delta\Theta>\theta_0$.

For a trapezoidal vertical beam profile, with base width $2\Delta X_0$, top width $2\lambda\Delta X_0$ ($\lambda<1$), and unit height,

$$\mathcal{F}(x_0)=\begin{cases}1, & |x_0|\leq\lambda\Delta X_0 \quad (14a)\\ \dfrac{1}{1-\lambda}\left[1-\dfrac{x_0}{\Delta X_0}\right], & \lambda\Delta X_0<x_0\leq\Delta X_0 \quad (14b)\end{cases}$$

and the integration over azimuthal angles yields

$$\gamma(\theta,E_0,V)=\begin{cases}1, & 0\leq\theta\leq\lambda\theta_0 \quad (15a)\\ \dfrac{2}{(1-\lambda)\pi}\left\{\dfrac{\pi}{2}-\lambda\arcsin\left[\lambda\dfrac{\theta_0}{\theta}\right]-\left[\left[\dfrac{\theta}{\theta_0}\right]^2-\lambda^2\right]^{1/2}\right\}, & \lambda\theta_0<\theta\leq\theta_0 \quad (15b)\\ \dfrac{2}{(1-\lambda)\pi}\left\{\arcsin\left[\dfrac{\theta_0}{\theta}\right]-\lambda\arcsin\left[\lambda\dfrac{\theta_0}{\theta}\right]+\left[\left[\dfrac{\theta}{\theta_0}\right]^2-1\right]^{1/2}-\left[\left[\dfrac{\theta}{\theta_0}\right]^2-\lambda^2\right]^{1/2}\right\}, & \theta_0<\theta\leq\Delta\Theta\ . \quad (15c)\end{cases}$$

For a trapezoidal horizontal beam profile, with base width $2\Delta Z_0$, top width $2\mu\Delta Z_0$ ($\mu<1$), and unit height,

$$\mathcal{G}(z_0)=\begin{cases}1, & |z_0|\leq\mu\Delta Z_0 \quad (16a)\\ \dfrac{1}{1-\mu}\left[1-\dfrac{|z_0|}{\Delta Z_0}\right], & \mu\Delta Z_0<|z_0|\leq\Delta Z_0\ . \quad (16b)\end{cases}$$

Defining

$$d=z_D+\mu\Delta Z_0 \tag{17}$$

we obtain

$$\mathcal{G}(z_D-\alpha L+\alpha L\cos\theta)=1, \quad 0\leq\theta\leq\left[\frac{2\theta_0 d}{\Delta X_0}\right]^{1/2} \tag{18a}$$

$$\mathcal{G}(z_D-\alpha L+\alpha L\cos\theta)=1+\frac{d}{(1-\mu)\Delta Z_0}-\frac{\theta^2\Delta X_0}{2\theta_0(1-\mu)\Delta Z_0}, \quad \left[\frac{2\theta_0 d}{\Delta X_0}\right]^{1/2}<\theta\leq\Delta\Theta \tag{18b}$$

and then $\Gamma(\theta,E,V)$ can be computed using Eqs. (11), (15), and (18). Figure 5 shows two examples, calculated for CsBr. It can be seen that the effect of Γ is to suppress the forward contribution to the scattering cross section, as expected.

IV. RESULTS

We have measured the effective cross section $\Delta\sigma$ for the scattering-out of alkali-halide molecules by electrons on CsCl, RbBr, RbCl, and KI at energies between 3 and 22.5 eV. The results are presented in Table I.[44]

Each value of $\Delta\sigma$ presented in Table I is the average of

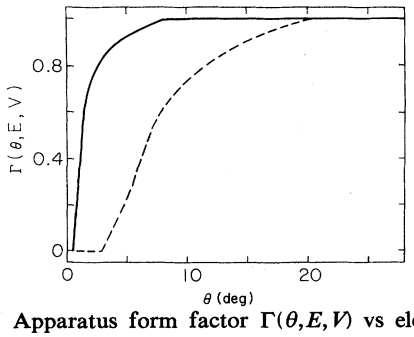

FIG. 5. Apparatus form factor $\Gamma(\theta,E,V)$ vs electron polar scattering angle. $M=212.8$ amu. Solid line: $E=5$ eV, $V=525$ m/sec. Dashed line: $E=22.5$ eV, $V=199$ m/sec.

TABLE I. Effective cross sections $\Delta\sigma$ for the scattering of electrons by alkali-halide molecules.

Energy (eV)	CsBr[a]	KI	CsCl	RbBr	RbCl
1.0	214.0± 16.0				
2.0	129.0± 10.0				
3.0	112.0± 8.0	181.0± 17.0			
3.5			397.0± 19.0	460.0± 30.0	538.0± 23.0
4.0	94.4± 5.0	157.0± 9.0			
5.0	87.0± 4.8	119.0± 7.0	323.0±24.0	349.0±20.0	431.0±24.0
7.5	72.3± 4.6	105.0±11.0	182.0±15.0	230.0±14.0	268.0±23.0
10.0	70.2± 4.0	79.0± 4.4	123.0±12.0	150.0±10.0	187.0±16.0
12.5	68.6± 3.1	68.7± 3.6	97.2± 6.7	100.0± 5.0	124.0±10.0
15.0	63.7± 3.6	76.7± 5.3	86.5± 5.6	83.4± 4.0	100.0±9.0
17.5	62.2± 3.1	62.1± 3.0	74.7± 4.0	80.3± 3.9	79.4±7.1
20.0	58.5± 2.5	73.7± 4.7	71.4± 3.4	71.4± 3.0	70.0±5.8
22.5	57.9± 3.2		65.6± 3.3	71.0± 4.3	66.7± 4.7

[a]The values previously given by B. Jaduszliwer, A. Tino, P. Weiss, and B. Bederson [Phys. Rev. Lett. **51**, 1644 (1983)] are affected by an error in beam-geometry parameters. The present table contains the correct values.

many data runs at that energy. The indicated errors represent a combination of statistical errors (one standard deviation from the mean) and conservative estimates of possible systematic errors. The most likely sources of systematic errors are the uncertainties in the determination of the height of the interaction volume, h, taken to be equal to the height of the slits defining it, known to be better than 1%, and the use of the temperature of the external surface of the nozzle to determine the molecular velocity distribution in the beam.

The differential cross sections for the scattering of electrons by alkali-halide dimers and monomers will differ most dramatically for small-angle scattering, because the dimers do not have a permanent electric dipole moment.[41] Thus, we may expect the presence of a small fraction of dimers in the beam to complicate the analysis of the small-angle distribution of scattered electrons (or recoiled molecules). But in our experiment, that small-angle contribution is suppressed by the scattering-out form factor $\Gamma(\theta,E,V)$, as discussed in Sec. III, so that the presence of a 1% or 2% fraction of dimers should not contribute significantly to the overall error.

In order to compare our results with theory, the calculated quasielastic differential cross sections have to be folded with the form factor $\Gamma(\theta,E,V)$, using the following prescription, as discussed in the previous section:

$$\Delta\sigma=\frac{2\pi}{I_\eta I_\zeta}\int_{-3}^{3}d\eta\exp(-\eta^2/2)\times\int_{0.1}^{2.5}d\zeta\,\zeta^2\exp(-\zeta^2)\times\int_0^{\pi}\Gamma(\theta,\theta_0)\sigma(E_0+\epsilon\eta,\theta)\times\sin\theta\,d\theta \tag{19}$$

with the reduced velocity $\zeta=(M/2kT)^{1/2}V$, and the reduced energy $\eta=(E-E_0)/\epsilon$. E_0 is measured in eV, and $\epsilon=0.28$ eV is the half-width at half maximum of the electron energy distribution, which is quite close to Gaussian. The molecular velocity distribution is assumed to be a modified (V^3) Maxwellian; the results are not very sensitive to the details of the distributions. I_η and I_ζ are the normalization integrals,

$$I_\eta=\int_{-3}^{3}\exp(-\eta^2/2)d\eta\ , \tag{20a}$$

$$I_\zeta=\int_{0.1}^{2.5}\exp(-\zeta^2)d\zeta\ . \tag{20b}$$

The cutoff angle θ_0, which represents the overall angular resolution of the measurement, is given by

$$\theta_0=8.56\times10^{-3}\mathcal{M}^{1/2}\zeta/(E_0+\epsilon\eta)^{1/2} \tag{21}$$

where $\mathcal{M}$ is the molecular weight. $\Gamma(\theta,\theta_0)$ is obtained using Eqs. (11) with $\Delta\Theta$ given by

$$\Delta\Theta=\begin{cases}1.12\theta_0^{1/2} & \text{(for CsBr)} \quad (22a)\\ 1.38\theta_0^{1/2} & \text{(for all others)} \quad (22b)\end{cases}$$

$\Gamma(\theta,\theta_0)$ given by Eqs. (15) with $\lambda=0.317$, and $\mathcal{G}(z_D-\alpha L\cos\theta)$ given by

$$\mathcal{G}=1-0.797\theta^2/\theta_0 \quad \text{(for CsBr, } 0\le\theta\le\Delta\Theta) \tag{23a}$$

$$\mathcal{G}=1 \quad \text{(for all others, } 0\le\theta\le0.782\theta_0^{1/2}) \tag{23b}$$

$$\mathcal{G}=1.451-0.762\theta^2/\theta_0 \quad \text{(for all others, } 0.782\theta_0^{1/2}\le\theta<\Delta\Theta)\ . \tag{23c}$$

The difference between the prescription for CsBr and for the other alkali halides studied in these experiments is due to a slightly different collimating slit in front of the electron gun, and a slightly different positioning of the detector with respect to the beam axis.

If the differential cross section does not vary too much over a few tenths of an eV about E_0, integrating over η becomes unnecessary, because Γ does not vary rapidly with electron energy. In that case, $I_\eta=1$, and $\eta=\epsilon=0$ in Eqs. (19) and (21).

We have performed the integration in Eq. (19) for the differential cross sections obtained using the RPDFBA,

and the ones calculated by Dickinson[31] using classical perturbation theory.

The RPDFBA cross section is given,[24] in atomic units, by

$$\sigma_{jj'}(\theta,k^2)\simeq\frac{2}{3}\frac{D^2}{k^2}\frac{j_>}{2j+1}\frac{1}{1-\cos\theta+\Delta}\ , \tag{24}$$

where $\Delta=\frac{1}{8}(\Delta E/E)^2$; $\Delta E=2hBj_>$, where B is the rotational constant of the molecule. $j'=j\pm1$, and $j_>$ is the larger of j and j'. For CsBr, $B\simeq1.08\times10^9$ sec^{-1}, and in the conditions of our experiment, where the largest j making significant contributions is about 200, $\Delta E\leq1.7\times10^{-3}$ eV. For an electron energy of about 5 eV, $\Delta\simeq1.5\times10^{-8}$; if $\theta\geq1.5\times10^{-3}$ rad, Δ can be neglected. Similar results are valid for the other alkali halides studied in the present paper. Since the scattering-out form factor $\Gamma(\theta,E,V)$ suppresses the very small θ contribution, we can safely neglect Δ in Eq. (24).

The observed differential cross section will be the sum of $\sigma_{jj'}(\theta,k^2)$ over the allowed values of j', averaged over the Boltzmann distribution of initial j states in the beam. With Δ neglected in Eq. (24) and $j'=j\pm1$, it is easy to show that, for θ not too small,

$$\sum_{j'}\sigma_{jj'}(\theta,k^2)\simeq\frac{2}{3}\frac{D^2}{k^2}\frac{1}{1-\cos\theta}\ \text{(a.u.)} \tag{25}$$

which is independent of j, so there is no need to perform the averaging over the initial j distribution. The RPDFBA result for the observed cross sections is, then,

$$\sigma(E,\theta)=\frac{1.966D^2}{E\sin^2(\theta/2)}\times10^{-17}\ \text{cm}^2\quad(\theta\geq1.5\times10^{-3}) \tag{26}$$

with E in eV and D in debyes. Dickinson[33] divided the scattering into three angular regions: small angles ($\theta\leq\Theta_1$), intermediate angles ($\Theta_1<\theta\leq\Theta_2$), and large angles ($\Theta_2<\theta$). In the small-angle region (large impact parameters, weak interaction with the target) he applies the RPDFBA. For intermediate angles he performs a classical perturbation theory calculation, and the transition angle Θ_1 is chosen using uncertainty principle considerations. At low energies, for $\theta\geq\Theta_2=60°$ he keeps the differential cross section constant at the 60° value; for high enough energies, he performs hard sphere scattering on a molecular core of radius equal to the internuclear separation R; Θ_2 decreases as the electron energy E increases. Dickinson's results are presented as very simple analytical functions of E and θ, involving the electric dipole moments and internuclear separations of the targets.

Our experimental results are compared with calculated values of effective cross sections $\Delta\sigma$ in Fig. 6. In every case, the top curve is the RPDFBA result, and the bottom curve Dickinson's. The relevant molecular data are

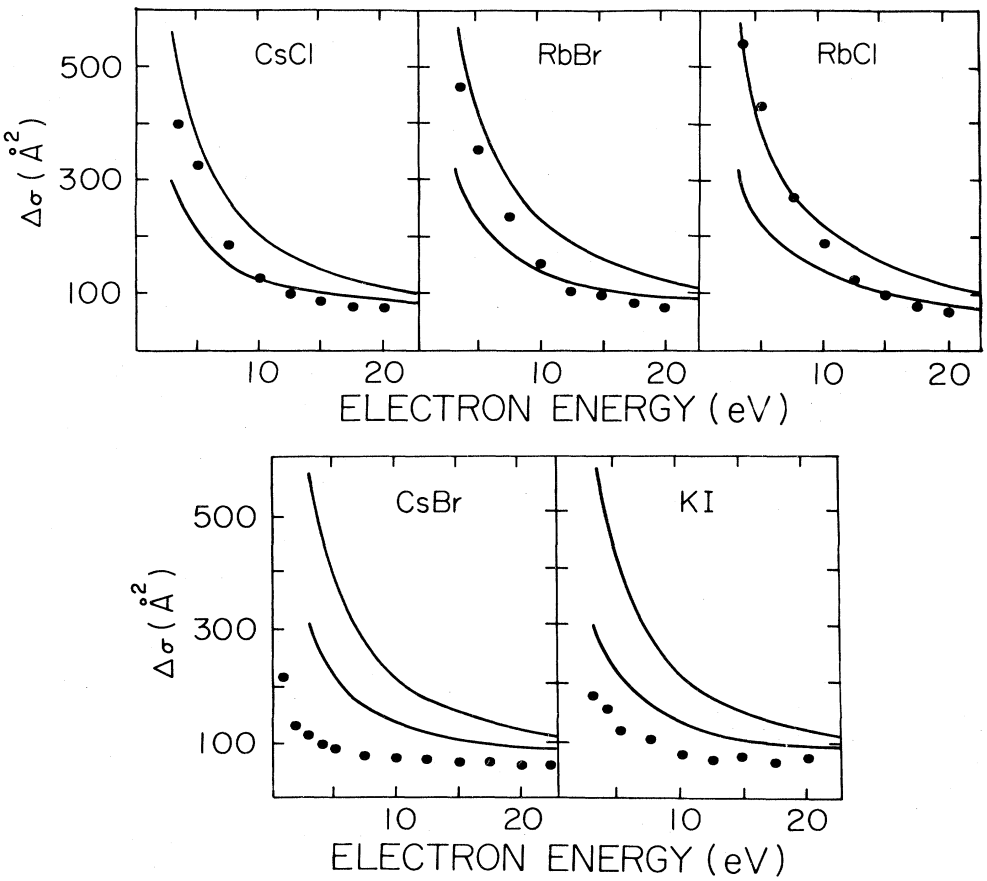

FIG. 6. Effective cross sections for electron scattering by alkali-halide molecules. Dots, present work; top curves, calculated values, using the RPDFBA differential cross sections; bottom curves, calculated values, using Dickinson's (Ref. 33) differential cross sections.

TABLE II. Molecular constants for some alkali halides.

Molecule	Mass (amu)	Dipole moment[a] (debye)	Internuclear separation[a] (Bohr radii)
CsBr	212.8	10.82	5.8058
CsCl	168.4	10.39	5.4924
KI	166.0	10.82	5.7597
RbBr	165.4	10.86	5.5649
RbCl	120.9	10.51	5.2666

[a]K. P. Huber and G. Herzberg, *Constants of Diatomic Molecules* (Van Nostrand Reinhold, New York, 1979).

presented in Table II.

Since our experiment suppresses the very large small-angle contribution to the total cross section, it is a sensitive test of the theory at larger angles, where the details of the interaction between projectile and target become more important. In general at the higher energies our results are lower than (but quite close to) Dickinson's (and, *a fortiori*, lower than the RPDFBA). At lower energies, our results can be substantially lower than Dickinson's, as for CsBr and KI, or become as high as the RPDFBA, as for RbCl.

There is nothing in the present results that contradicts the widely held opinion that the RPDFBA differential cross sections are quite accurate at small angles. If that assumption is correct, then, judging from the difference between the RPDFBA and experimental values for $\Delta\sigma$, the total cross sections calculated using the RPDFBA are too high by 10% to 20%.

ACKNOWLEDGMENTS

This work was supported by the Office of Basic Energy Sciences, Division of Chemical Sciences, U. S. Department of Energy. We thank Dr. Phyllis Weiss for her help during the course of this work.

*Present address: AT&T Bell Laboratories, Holmdel, NJ 07733.

[1]H. S. W. Massey, Proc. Cambridge Philos. Soc. **28**, 99 (1931).
[2]V. A. Bailey and W. A. Duncanson, Philos. Mag. **10**, 145 (1930).
[3]J. L. Pack, R. E. Voshall, and A. V. Phelps, Phys. Rev. **127**, 2084 (1962).
[4]G. S. Hurst, J. A. D. Stockdale, and L. B. O'Kelley, J. Chem. Phys. **38**, 2572 (1963).
[5]A. Christophorou, G. S. Hurst, and A. Hadjiantoniou, J. Chem. Phys. **44**, 1506 (1966).
[6]N. Hamilton and J. A. D. Stockdale, Aust. J. Phys. **19**, 813 (1966).
[7]R. D. Hake and A. V. Phelps, Phys. Rev. **158**, 70 (1967).
[8]J. S. Townsend and V. A. Bailey, Philos. Mag. **42**, 873 (1921).
[9]S. Altshuler, Phys. Rev. **107**, 114 (1957).
[10]M. H. Mittleman and R. E. von Holdt, Phys. Rev. **140**, A276 (1965).
[11]K. Takayanagi, J. Phys. Soc. Jpn. **21**, 507 (1966).
[12]O. H. Crawford, J. Chem. Phys. **47**, 1100 (1967).
[13]O. H. Crawford, A. Dalgarno, and P. B. Hays, Mol. Phys. **13**, 181 (1967).
[14]J. M. Lévy-Leblond and J. P. Provost, Phys. Lett. **26B**, 104 (1967).
[15]O. H. Crawford, Proc. Phys. Soc. London **91**, 279 (1967).
[16]K. Takayanagi and Y. Itikawa, J. Phys. Soc. Jpn. **24**, 160 (1968).
[17]A. Dalgarno, O. H. Crawford, and A. C. Allison, Chem. Phys. Lett. **2**, 381 (1968).
[18]C. Bottcher, Mol. Phys. **19**, 193 (1970).
[19]W. R. Garrett, Phys. Rev. A **3**, 961 (1971).
[20]W. R. Garrett, Mol. Phys. **20**, 751 (1971).
[21]W. R. Garrett, Phys. Rev. A **4**, 229 (1971).
[22]Y. Itikawa, Phys. Rep. **46**, 117 (1978).
[23]N. Lane, Rev. Mod. Phys. **52**, 29 (1980).
[24]D. W. Norcross and L. A. Collins, in *Advances in Atomic and Molecular Physics,* edited by D. R. Bates and B. Bederson (Academic, New York, 1982), Vol. 18, pp. 241–397.
[25]R. C. Slater, M. G. Fickes, W. G. Becker, and R. C. Stern, J. Chem. Phys. **60**, 4697 (1974).
[26]W. G. Becker, M. G. Fickes, R. C. Slater, and R. C. Stern, J. Chem. Phys. **61**, 2287 (1974).
[27]R. C. Slater, M. G. Fickes, W. G. Becker, and R. C. Stern, J. Chem. Phys. **61**, 2287 (1974).
[28]M. G. Fickes and R. C. Stern, J. Chem. Phys. **60**, 4710 (1974).
[29]L. A. Collins and D. W. Norcross, Phys. Rev. A **18**, 467 (1978).
[30]M. R. H. Rudge, S. Trajmar, and W. Williams, Phys. Rev. A **13**, 2074 (1976).
[31]L. Vuskovic, S. K. Srivastava, and S. Trajmar, J. Phys. B **11**, 1643 (1978).
[32]L. Vuskovic and S. K. Srivastava, J. Phys. B **14**, 2677 (1981).
[33]A. S. Dickinson, J. Phys. B **10**, 967 (1977).
[34]J. Siegel, J. L. Dehmer, and D. Dill, J. Phys. B **14**, L441 (1981).
[35]B. Jaduszliwer, A. Tino, P. Weiss, and B. Bederson, Phys. Rev. Lett. **51**, 1644 (1983).
[36]B. Jaduszliwer, P. Weiss, A. Tino, and B. Bederson, preceding paper, Phys. Rev. A **30**, 1255 (1984).
[37]R. E. Collins, B. B. Aubrey, P. N. Eisner, and R. J. Celotta, Rev. Sci. Instrum. **41**, 1403 (1970).
[38]N. F. Ramsey, *Molecular Beams* (Oxford University, London, 1956), pp. 16–19.
[39]A. Kasdan, T. M. Miller, and B. Bederson, Phys. Rev. A **8**, 1562 (1973).
[40]B. Bederson and L. J. Kieffer, Rev. Mod. Phys. **43**, 601 (1971).
[41]R. Kremens, B. Jaduszliwer, B. Bederson, and J. A. D. Stockdale, in *Metal Bonding and Interaction in High Temperature Systems,* edited by J. L. Gole and W. C. Stwalley, Am. Chem. Soc. Symp. Ser. No. 179 (American Chemical Society, Washington, D.C., 1982), pp. 301–307.
[42]R. C. Miller and P. Kusch, J. Chem. Phys. **25**, 860 (1956).
[43]Otherwise, $\Delta\sigma$ equals the integral in Eq. (10) plus the total cross section for electronically elastic processes.
[44]In the preliminary report (Jaduszliwer *et al.*, Ref. 35) on electron scattering by CsBr, an error in beam-geometry parameters was found. The new, corrected values of $\Delta\sigma$ for CsBr are also given in Table I.